Volume 350, Issue 1, October 1, 2010

ISSN 0021-9797

Journal of COLLOID AND INTERFACE SCIENCE

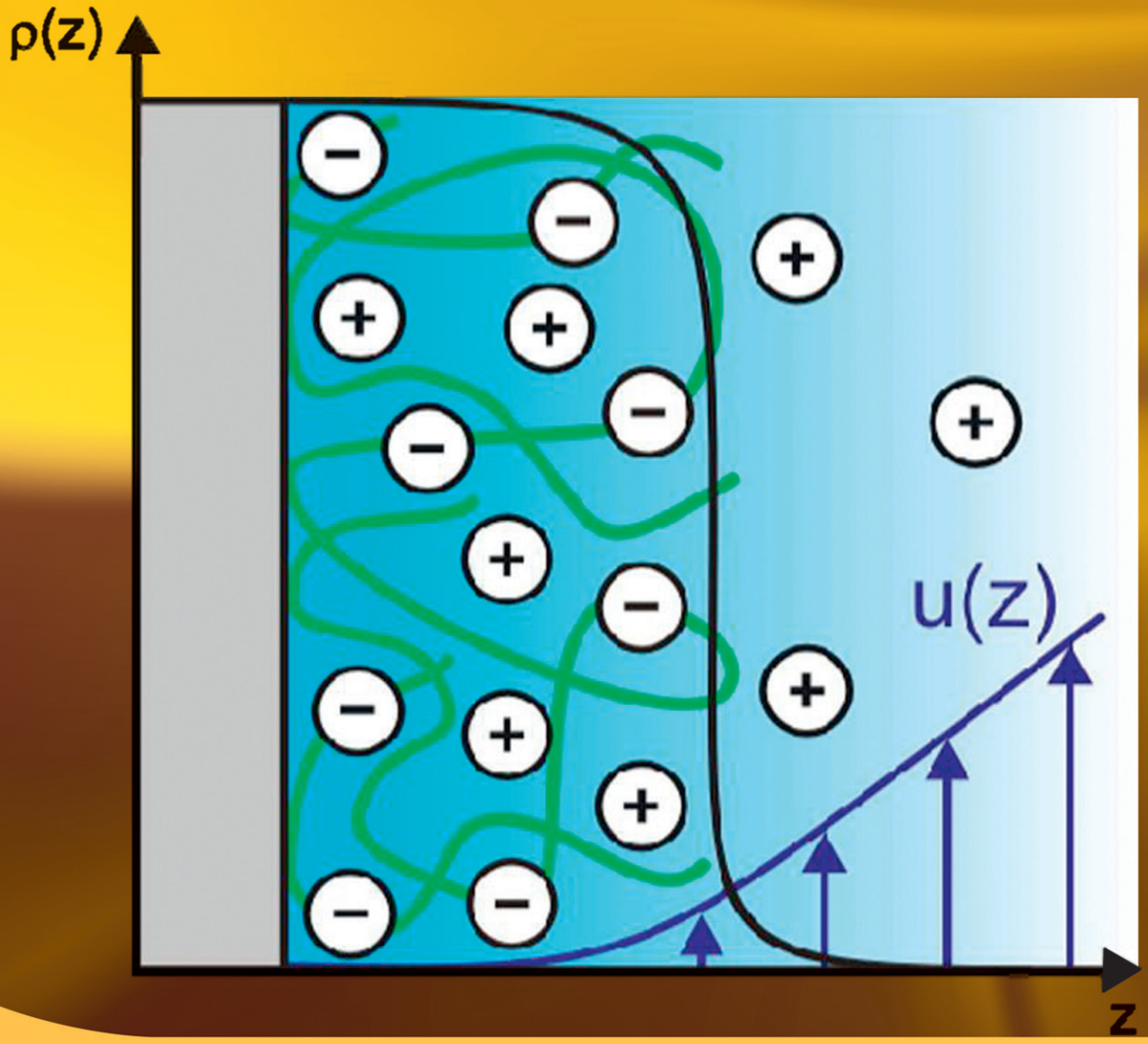

From Stanislav S. Dukhin et al. *pages 1–4*

www.elsevier.com/locate/jcis

Journal of Colloid and Interface Science 350 (2010) 186–193

Contents lists available at ScienceDirect

Journal of Colloid and Interface Science

www.elsevier.com/locate/jcis

Tailoring the wettability of polypropylene surfaces with halloysite nanotubes

Mingxian Liu [a,b], Zhixin Jia [a], Fang Liu [a], Demin Jia [a,*], Baochun Guo [a]

[a] College of Materials Science and Engineering, South China University of Technology, Guangzhou 510640, PR China
[b] Department of Materials Science and Engineering, Jinan University, Guangzhou 510632, PR China

ARTICLE INFO

Article history:
Received 29 April 2010
Accepted 17 June 2010
Available online 22 June 2010

Keywords:
Superhydrophobic
Polypropylene
Halloysite nanotube
Crystallization
Nanocomposite
Roughness

ABSTRACT

In this contribution, halloysite nanotubes (HNTs), a kind of natural hydrophilic nanoclay, are incorporated into polypropylene (PP) for tailoring the surface microstructures of the composites prepared by solution casting. HNTs act as heterogeneous nuclei for PP, which leads to the change of phase separation process during drying of the composites and consequently the microstructures of composite surfaces. Micro-papilla like hybrid spherulites with nanostructures are formed on the PP/HNTs composite surfaces. The rough surfaces demonstrate superhydrophobicity with a maximum water contact angle as nearly 170° and sliding angle of about 2°. The spherulites size, surface roughness, and wetting property of PP can be tuned by HNTs. HNTs can significantly improve the thermal degradation behavior of the composites which is attributed to the well-dispersed HNTs and the improved interfacial interactions by the nucleation effect. The present work provides an alternative routine for preparing polymer superhydrophobic surfaces via tailoring the surface microstructures by adding nanoparticles in a solution process.

1. Introduction

Superhydrophobic surface has attracted widely interests all over the world in recent years with evidence of the rapid increasing numbers of published papers on this issue [1–9]. This can be attributed to the unique wetting properties of these surfaces, such as extreme water repellency and self-cleaning. A water droplet on superhydrophobic surfaces keeps almost as a spherical shape with a contact angle larger than 150° and it can easily roll off when the surfaces are tilted. If there are dust on these surfaces, the rolling water droplets can bring them off and hence the surfaces can keep always clean. In nature, many plant and insects, such as lotus leaves [2], water strider's legs [7] and butterfly wings [10], exhibit surfaces with the superhydrophobic property. Generally, wettability of a solid is governed by both the chemical composition and geometrical microstructure of the surfaces. To mimic the topology of the natural water-repellent surfaces, artificial superhydrophobic surfaces are prepared by vast different techniques and materials [8,9]. These synthesized surfaces with unique wettability can be applied in many areas, such as the prevention of the adhesion of snow to antennas and windows, self-cleaning traffic indicators, antifouling coatings, the reduction of frictional drag on ship hulls, metal refining, stain-resistant textiles and cell motility. Although these artificial superhydrophobic surfaces are reported with excellent water-repellent property, most of them suffer from the drawbacks such as complicate procedures, expensive raw materials, and non-reproducible results. Therefore, exploiting a simple, flexible, and economic method for superhydrophobic surfaces is generally highlighted.

In 2003, Erbil et al. reported a simple approach for forming superhydrophobic surfaces with polypropylene (PP) via controlling phase separation by adding non-solvent [6]. The non-solvents act as precipitator to promote the phase separation process when PP solution is drying. Formation of porous surface with finer spherulites is found and the microstructures and wettability of the PP surfaces can be tuned by the non-solvents. Inspired by this result, other polymers such as polyethylene (PE) [11–13], polycarbonate (PC) [14,15], polystyrene (PS) [16], poly(vinyl chloride) (PVC) [17], and poly(L-lactic acid) (PLA) [18] were employed for fabrication of superhydrophobic surfaces using the controlled phase-separation method. For example, phase separation process can be induced by the non-solvents of ethanol, water or their mixtures and superhydrophobic surfaces of PE, PS, PC, PVC, or PLA are obtained. The non-solvents act as "seed" where the polymer chains tend to be absorbed in the phase separation process. For crystalline polymer systems, the role of non-solvents is like nucleation which can leads to the alignment and entanglement of polymer chains on the surfaces of nuclei. Although organic solvents are involved in the phase-separation method, it is a simple, effective, and flexible routine for fabrication polymer superhydrophobic surfaces. Recently, Rioboo et al. investigated the effect of the solution concentration and film thickness on the superhydrophobicity of various PP in detail [19]. However, such kinds of technologies were confined to neat polymers and never implemented in polymer composites.

Nanoparticles, such as carbon nanotubes (CNTs), nanoclays, and nanosilica, are incorporated into polymers for improving their performance or functions [20]. The introduction of nanoparticles can

* Corresponding author. Fax: +86 20 2223 6688.
E-mail address: psdmjia@scut.edu.cn (D. Jia).

0021-9797/$ - see front matter © 2010 Elsevier Inc. All rights reserved.
doi:10.1016/j.jcis.2010.06.047

significantly change the microstructures of polymer matrix which in turn leads to the changed properties of polymer materials. The nucleation of nanoparticles towards crystalline polymers is widely concerned due to their significance for both theoretical and practical values. For example, CNTs can induce transcrystalline or shish-kebab crystal of polyolefin via soft-epitaxy mechanism under proper condition [21,22]. Clay or nanosilica can also play the heterogeneous nucleating points role for various polymers [23–25]. Generally, the nucleation effect of nanoparticles results in finer crystals, faster crystallization process, and some times novel crystal forms. When the polymer composites are prepared by solution blending method, nanoparticles can accelerate the phase separation process during drying of the composites via nucleation. As a consequence, rough polymer surfaces can also be formed when one replaces the non-solvent with nanoparticles as nanoparticles can act as a special precipitator of polymer solutions. In the present paper, we used a kind of natural occurred inorganic nanotubes, halloysite nanotubes (HNTs), to tailor the surface microstructures of PP in a solution process. The heterogeneous nucleation of HNTs to PP was examined. Micro-papilla like hybrid spherulite with nanostructures was observed for the PP/HNTs composite surfaces. These rough surfaces demonstrate superhydrophobicity with a water contact angle higher than 160° and sliding angle less than 10°. The present work provides an example for tailoring the surface microstructures and wetting property of polymers by adding nanoparticles in a solution process.

2. Material and methods

2.1. Materials

Isotactic PP granules with tradename F401 were commercial products of Lanzhou Petrochemical Co. Ltd. The melt flow index was determined as 2.84 g/10 min (after ISO-1133: 1997(E)). The HNTs were mined from Yichang, Hubei, China. The elemental composition was determined by X-ray fluorescence (XRF) as follows (wt.%): SiO_2, 58.91; Al_2O_3, 40.41; Fe_2O_3, 0.275; TiO_2, 0.071. The Brunauer–Emmett–Teller (BET) surface area of the used HNTs was 50.4 m^2/g. HNTs were purified according to the Ref. [26]. The purified HNTs were with highly tubular morphology as shown in Fig. 1.

2.2. Methods

2.2.1. Preparation of PP/HNTs composites superhydrophobic surfaces

The superhydrophobic surfaces of PP/HNTs composites were prepared via solution casting method. A typical procedure was as follows: 0.6 g PP granules were dissolved completely in 30 mL xylene at 120 °C. Then dried HNTs powders were added to the solution under stirring and the temperature was kept at 120 °C. The PP/HNTs solutions were stirred for 30 min with a rotation rate of 800 rpm to completely disperse HNTs. Finally the solutions were casted on clean glass slides and dried at room temperature for 1–4 h. The final thickness of the formed film was around 50 μm. The content of HNTs was the weight ratio of HNTs to the total composites.

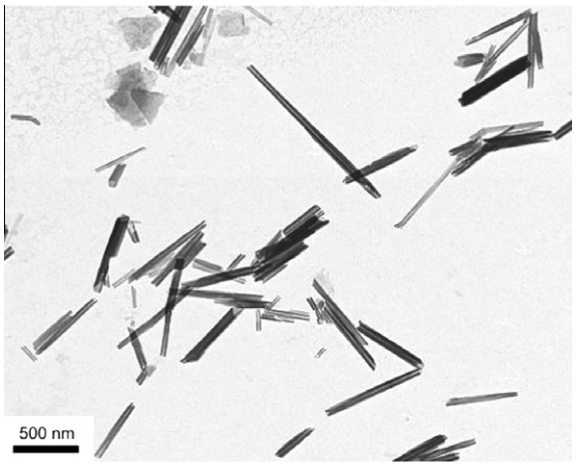

Fig. 1. Transmission electron microscope image of the used HNTs.

2.2.2. Characterization

Differential scanning calorimetry (DSC) data of neat PP and PP/HNTs composites were measured by TA Q20 using nitrogen as the purging gas. The samples were heated to 210 °C at the ramping rate of 40 °C/min. The samples were kept at 210 °C for 5 min to eliminate thermal history before they were cooled down to 40 °C at rate of 10 °C/min. The exothermic flows were recorded as a function of temperature. The crystallization onset temperature ($T_{c\ on}$) and peak temperature (T_c) were obtained from the curves by the TA Universal Analysis software.

The X-ray diffraction (XRD) patterns of PP and PP/HNTs composites were recorded by the Bruker D8 Advanced X-ray Diffractometer. The Cu Kα radiation source was operated at 40 kV power and 40 mA current. The patterns were recorded by monitoring those diffractions that appeared from 2° to 40°. The scanning speed was 1°/min.

The morphologies of the crystallites of PP and PP/HNTs composites were recorded with an Olympus BX41 polarized optical microscopy (POM). The PP and PP/HNTs composites thin films for POM observation were obtained by dropping their diluted solutions on clean glass slides and subsequently drying them in air.

The scanning electron microscopy (SEM) micrographs were taken with LEO1530 VP SEM machine. The samples were coated with a very thin layer of gold before observation.

To evaluate the effect of HNTs on the phase separation process, the weight loss experiments were performed. About 0.25 g PP solution or PP/HNTs solution was carefully dropped on glass slide which was placed on a balance. The initial weight was recorded. Due to the gradually evaporation of solvent, the weight decreased and the changed weights were recorded every 30 s. The initial concentration of the PP solution and PP/HNTs solution was same for comparing the total drying time.

To evaluate the surface roughness of PP and PP/HNTs composites, roughness measurement were performed using a BMT Expert3D analyzer. The 3D surface topography of the samples was recorded on the basis of the white-light interference theory. The scanning area for all the samples is 4 × 3 mm. The scanning point density was 300 point/mm. The area average roughness (S_a) for all the samples were obtained using the BMT measurement and evaluation software.

Water contact angle and sliding angle of the prepared surfaces were measured with KRUSS Drop Shape Analyzer DSA 100 instrument under room temperature. The data measurement of contact angle and slide angle for all the samples were repeated for five times to obtain reliable values. The volume of water droplet was 4 μL for the contact angles measurement. The contact angles were calculated by software according to the Laplace-Young model. The sliding angle values were the critical angle of the inclination of the surfaces when a 10 μL water droplet started to roll off.

XPS spectra of the PP/HNTs composites with 15% HNTs and 40% HNTs were recorded by Kratos Axis UltraDLD with an Aluminum (mono) Kα source (1486.6 eV). The atom ratio values were calculated by integration of the area for the corresponding peaks by software.

Thermogravimetric analysis (TGA) for all the samples were carried out under air atmosphere with TA Q5000 at a heating rate of 10 °C/min from room temperature to 600 °C.

3. Results and discussion

3.1. Nucleation effect of HNTs toward PP

Generally, nanoparticles influence the crystallization process of polymers by acting as heterogeneous nuclei. This effect leads to the increase in nucleation and crystallization rate. As a consequence, higher crystallization temperatures and finer spherulites are obtained than those for neat polymer [20,23]. To illustrate the nucleation effect of HNTs toward PP, DSC measurements for neat PP and its composites were firstly performed. Fig. 2 shows the crystallization curves of the PP/HNTs composites with different HNTs content. Table 1 summarizes the DSC data and calculated crystallinity for PP/HNTs composites. From Fig. 2 and Table 1, it is clear that both crystallization onset temperature and crystallization peak temperature increase consistently with HNTs content. Meanwhile, the crystallinities of composites are considerably higher than that for neat PP. The observed effects are attributed to the nucleating effect of HNTs during crystallization process. It also should be noted that the present DSC results are quite different from our previous reported PP/HNTs composites which are prepared by melting mixing [25]. For the PP/HNTs composites with high HNTs loadings prepared by melting mixing, the crystallization peak temperature did not increase continuously. This difference comes from different dispersion states of HNTs and crystalline type of PP. For the composites prepared by melting mixing, the dispersions of HNTs become poor at relatively high HNTs content (above 20 wt.%) and this depresses the increase in the crystallization peak temperature. In addition, beta crystals of PP are formed in the PP/HNTs composites during the melting mixing process. Comparing with the composites prepared by melting mixing, dispersion of HNTs is supposed to be better for the composites prepared by solution mixing and no beta crystals are formed as illustrated by the XRD result shown in Fig. 3. The peaks at 2θ values of 14°, 16.7°, and 18.6° are assigned to the (1 1 0), (0 4 0), and (1 3 0) reflections of α phase for PP, respectively, [27]. No peak corresponding to β phase was observed for all samples. The diffraction peaks around 12° for the PP/HNTs composites are assigned to layer spacing of HNTs of 7.37 Å. The nucleation effect of HNTs to other polymers, such as polyvinyl alcohol [28] and polyamide [29], has also been suggested.

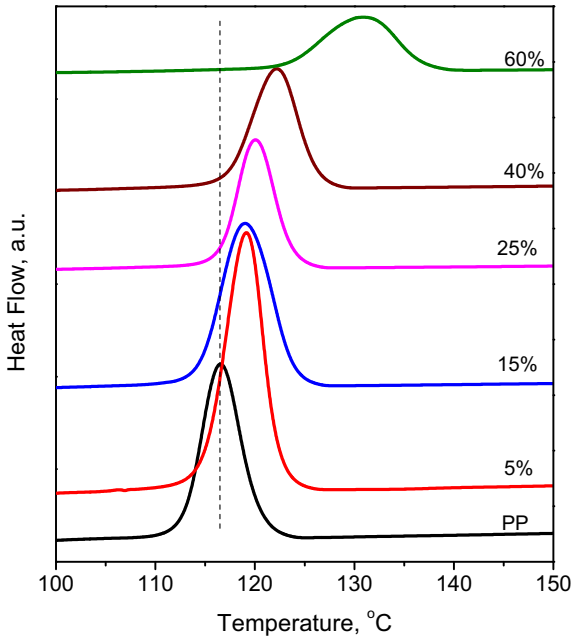

Fig. 2. DSC cooling curves for the PP and PP/HNTs composites.

Table 1
Data of PP and PP/HNTs composites from DSC measurement and the calculated crystallinity.

Samples	$T_{c\ on}$ (°C)	T_c (°C)	ΔH (J/g)	Crystallinity (%)
Neat PP	120.5	116.6	71.54	34.2
5% HNTs	122.4	119.2	77.65	39.1
15% HNTs	123.9	119.0	68.97	38.8
25% HNTs	123.7	120.1	64.04	40.9
40% HNTs	126.3	122.3	53.92	43.0
60% HNTs	136.8	130.9	41.82	50.0

POM was used to further demonstrate the nucleating effect of HNTs. A spherulitic morphology is observed for all the samples as shown in Fig. 4. These spherulites link each other to form a cluster of grape especially for neat PP sample. The size of the PP spherulites formed from solution is much smaller than that formed by molten. For a typical PP spherulite formed by molten, the diameter is larger than 100 μm [23]. The diameter of the present formed spherulites for PP is only about 5 μm. The significantly reduced crystal size is attributed to the interactions between PP and the solvent during drying of the composites. It also can be seen that the spherulite size of PP sharply decreases with the addition of HNTs due to above-mentioned nucleation effect. There are two predominant factors that affect the size of the spherulites: the thermodynamics condition such as crystallization temperature and crystallization time and the number of heterogeneous nucleation points. In the present study, HNTs are considered as the heterogeneous nucleation points for PP chain. Due to the small diameters of HNTs, the tubes can be considered as rigid macromolecules; hence the polymer chains prefer to absorb and align on HNTs surface. This mechanism can be attributed to "soft epitaxy", wherein strict lattice matching is not required. As the thermodynamic conditions are considered as similar for PP and PP/HNTs solutions, when a polymer starts to crystallize onto HNTs surface, geometric confinement is the major factor affecting the size of the spherulites. HNTs can prevent PP from growing into large size spherulites from the PP/HNTs solutions due to the significantly increased numbers of nucleation points. As a consequence, the decreased PP spherulite size for PP/HNTs composites is obtained. The finer spherulites are benefit for the improvement of surface roughness of the composites which in turn enhance the superhydrophobicity of PP as illustrated below. For the composites with relatively low filler content (lower than 40 wt.%), no HNTs aggregate are visible due to the good dispersion state of HNTs in the matrix. However, in Fig. 4c, some HNTs aggregates within several micrometers (the colorized irregular parts) are observed

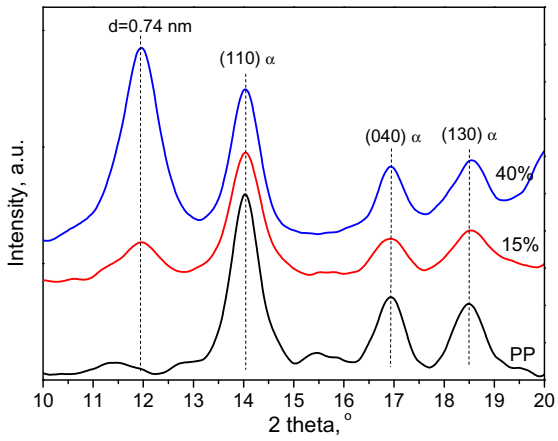

Fig. 3. XRD patterns of neat PP and PP/HNTs composites with indicating HNTs content.

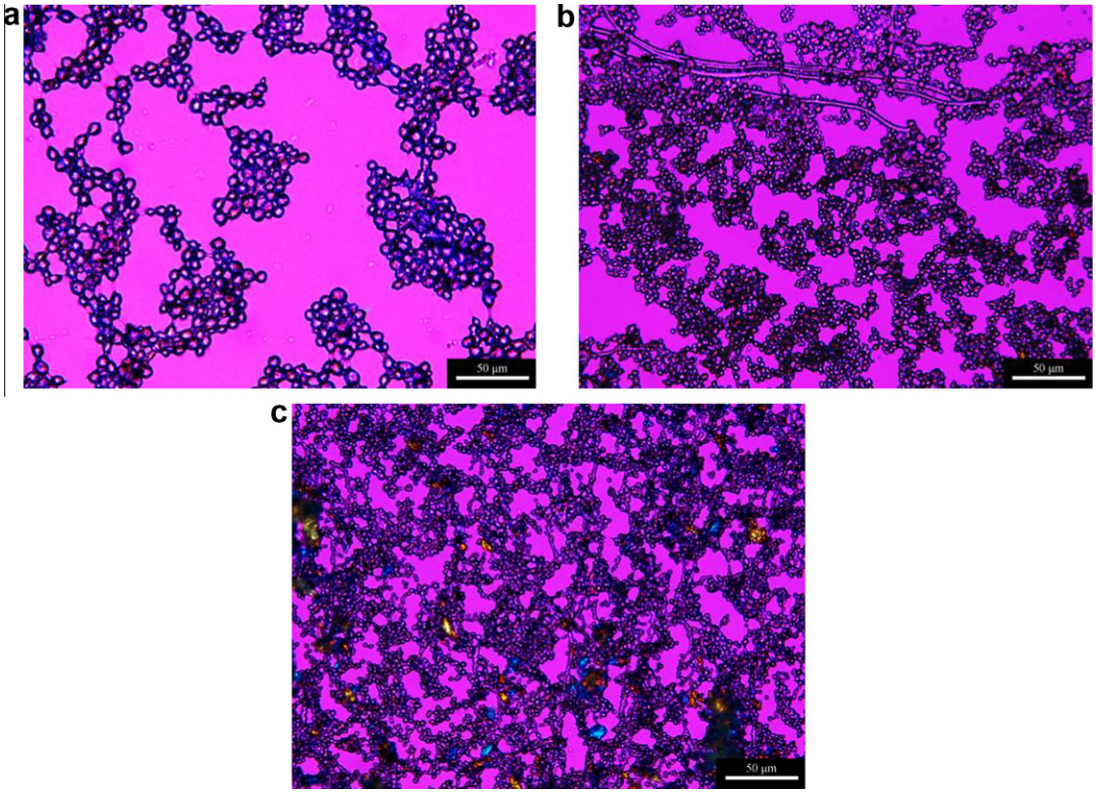

Fig. 4. POM photos of PP and PP/HNTs composites: (a) neat PP; (b) 15% HNTs; and (c) 40% HNTs.

in the composites with relatively high HNTs content. The hydrophilic HNTs aggregates may be exposed on the surface of composites which are detrimental to the hydrophobicity of the composites which will be illustrated below.

The decreased spherulite dimension of PP by HNTs was further verified by SEM. Fig. 5 shows the SEM photos of PP and PP/HNTs composite surfaces. It is clear that the PP and PP/HNTs composites surfaces are composed of interconnected spherulites whose surfaces are very rough. Voids are clearly visible between the spherulites on the rough surfaces which can enclose large volume of air and benefit for the improvement of hydrophobicity especially lowering the sliding angles. Consistent with the POM results, the dimension of PP spherulites gradually decreases by HNTs. The composite samples possess much more spherulites than PP does in the photos at same magnification. This result further confirms the nucleation effect of HNTs toward PP. Using the controllable phase-separation method by adding non-solvents, PP surfaces with similar morphological characteristic can also be obtained [6,30]. The decreased spherulite dimension by HNTs can lead to improvement of the surface roughness of PP. Fig. 6 compare the R_a curves of PP and PP/HNTs composites. From Fig. 6, it is clearly seen that the R_a and the peak to valley distance for the PP/HNTs composite surfaces are substantially increased comparing with those for neat PP surface. For example, the R_a of the composite with 15% HNTs is 6.05 μm, which is 32% higher than that of PP surface. As a comparison, the roughness R_a of blank glass substrate is only 34 nm. The improvement of the roughness indicates that more air can be trapped in these surfaces, which is critical for lowering the sliding angle for superhydrophobic surfaces.

The weight loss measurement also shows the nucleation effect of HNTs for PP. Fig. 7 shows the weight variation when PP and PP/HNTs solutions are exposed in air. It can be seen the total drying time of the coatings becomes shorter with the addition of HNTs. For PP solution, the complete drying time is about 17 min, while it shorten to 13 min for the composites with 40% HNTs. This can be explained by that HNTs can accelerate the phase separation process via acting as heterogeneous nuclei. Compared with the PP solution, the solvent evaporates more rapidly for the PP/HNTs solutions. In summary, all the experiment results show the nucleation effect of HNTs toward PP. The nucleation effect leads to the change of crystallization rate, crystallinity, and spherulite size. As a consequence, the surface roughness of PP is enhanced by HNTs.

3.2. Superhydrophobic property of PP/HNTs composites

PP is a kind of hydrophobic material because of no polar groups in its chemical composition. Due to PP's balanced physical and chemical properties, nontoxicity, and low cost, it has been widely used in many areas such as home appliances, automotive, and package films [27]. Therefore, the surface wettability is critical for its practical applications. To evaluate the hydrophobic properties of PP and PP/HNTs composites, water contact angles and sliding angles of their surfaces were determined. Fig. 8 shows the variation of contact angles of PP/HNTs composites surfaces. Without HNTs, PP can form rough surface with a water contact angle of about 160°. The contact angles increase when the HNTs are present in the composites but the content is lower than 60%. The maximum contact angle for the PP/HNTs composites is determined as nearly 170° with 15% HNTs. This is attributed to the change of surface microstructures of the composites by HNTs via nucleation effect during drying of the composites. No naked HNTs are exposed on the surfaces of PP/HNTs composites with relative low HNTs content as shown in Table 2. Carbon element is the dominated element for the PP/HNTs composites surfaces with 15% HNTs content. A small quantity of oxygen and silicon element originates from the impurities. The XPS result indicates that HNTs are buried inside the PP spheres during the rapid phase separation of PP from the solution. Overloading HNTs causes slightly decreased hydrophobicity of PP

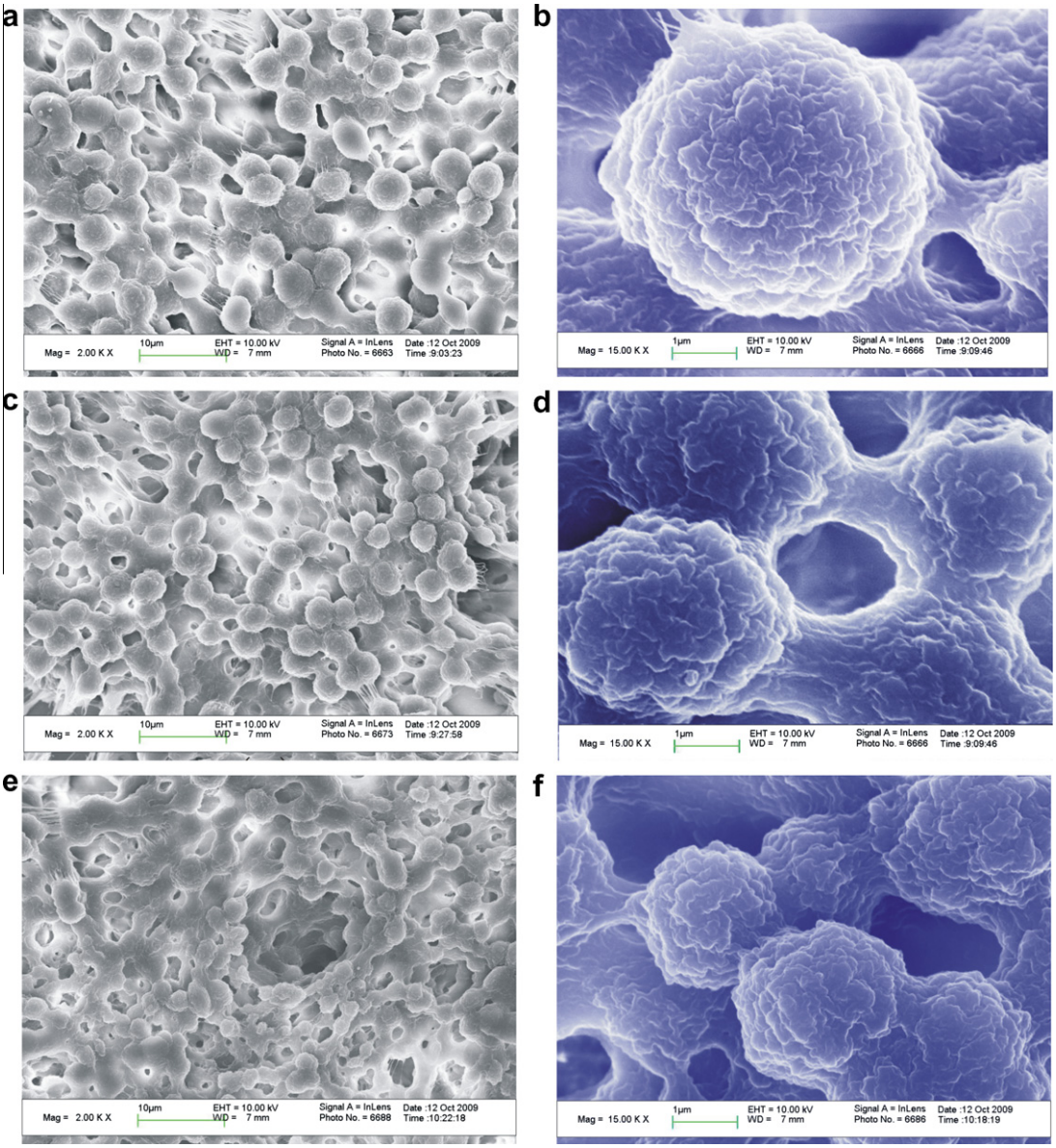

Fig. 5. SEM photos of PP and PP/HNTs composites: (a) and (b) neat PP; (c) and (d) 15% HNTs; (e) and (f) 40% HNTs.

composites, although they have relative high surface roughness as illustrated above. For example, the composites with 60% HNTs show a water contact angle of 153°. This is attributed to the emergence of HNTs aggregates on the composite surfaces with high HNTs content as revealed by the above POM results and the XPS results in Table 2. A large number of silicon and aluminum element is detected for the surface of the PP/HNTs composites with 60% HNTs, indicating the presence of naked HNTs aggregates. These hydrophilic aggregates are, of course, detrimental for the hydrophobicity of the surfaces.

Superhydrophobic surfaces, such as lotus leaf, do not only demonstrate a high water contact angle, but also low sliding angle. The low sliding angle allows them to be cleaned as the dirt on their surfaces can be removed by the rolling water droplets. Fig. 8 compares the sliding angles of neat PP with PP/HNTs composites. It can be seen the sliding angles for all the samples are lower than 10°. Addition of HNTs to PP leads to decrease in sliding angles when the content of HNTs is below 25%. Then the sliding angles of the surfaces increase slightly. Nevertheless, the sliding angles for all the samples are acceptable for the purpose of self-cleaning. The wettability experiment results indicate the prepared surfaces can be applied as protective coatings on various substrates with self-cleaning functions. This approach for preparing surperhydrophobic surfaces with polymer composites is simple, economic, and flexible. The idea for using nanoparticles of tailoring the microstructures and wettability of polymer surfaces can also be adopted in other polymer systems. One drawback for the prepared superhydrophobic surfaces is that they are opaque due to the crystallization of PP matrix.

3.3. Mechanism for the superhydrophobicity of PP/HNTs composites

According to the well-known Wenzel model describing the contact angle on a rough surface, the hydrophobicity of a surface is related to the surface roughness [31]. Therefore, obtaining a rough surface is critical for preparing PP superhydrophobic surfaces. The method of adding non-solvents to polymer solutions introduced by Erbil et al. is effective for producing the surface roughness of polymer surfaces and thus the superhydrophobic polymer surfaces can be obtained [6]. The sliding angle of a superhydrophobic surface can often be explained according to the Cassie–Baxter model. In the Cassie–Baxter model, the superhydrophobic surface

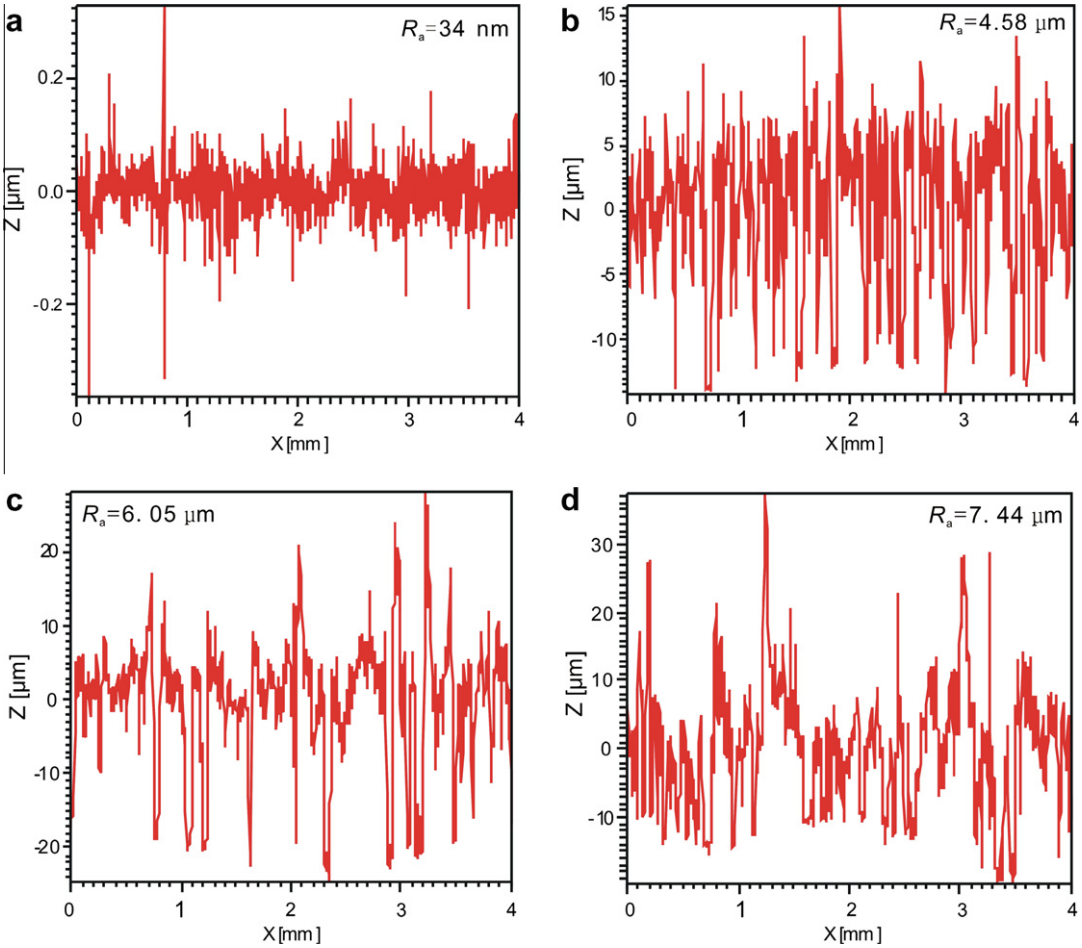

Fig. 6. Roughness curves of blank glass (a), neat PP (b), PP/HNTs composite with 15% HNTs (c), and with 40% HNTs (d).

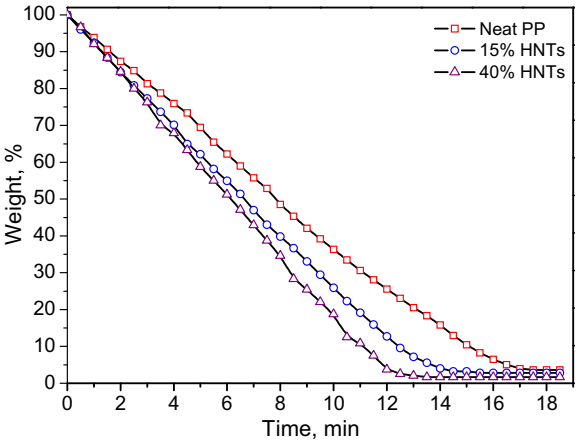

Fig. 7. Weight change curves for drying the PP and PP/HNTs solution at room temperature.

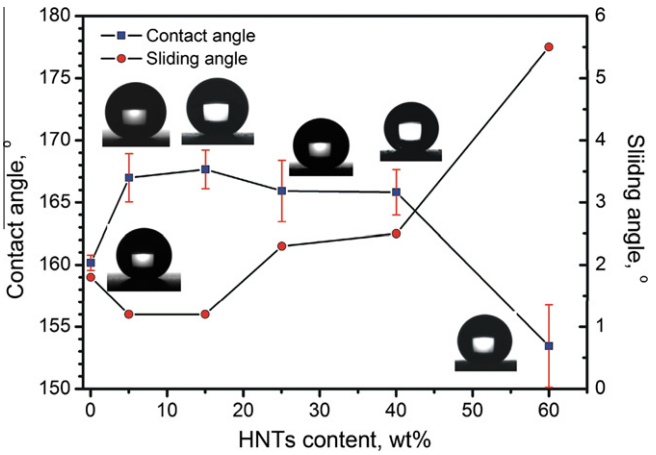

Fig. 8. Contact angles and sliding angles of the PP and PP/HNTs composite surfaces.

is considered as "composite" surfaces which are composed of solid and air [32]. The more air is enclosed for the rough surface, the lower the sliding angle is. For the present systems, the rough surfaces of PP are formed during drying of the solutions. Addition of HNTs leads to increasing in surface roughness due to their nucleation ability for PP. The combination of SEM and roughness measurement results demonstrates the increased roughness by HNTs. The high magnification SEM photos of PP and PP/HNTs composite,

Table 2
XPS atomic content (At.%) for the PP/HNTs composites with different HNTs content.

Atom	15% HNTs	60% HNTs
C	90.70	22.48
O	6.92	45.14
Si	1.39	17.34
Al	–	14.29

as shown in Fig. 5, confirms the formation of the micro-papilla like structures for both neat PP and the composite surfaces. More importantly, fine nanostructures are formed on the surfaces of the micro-papilla structures. Since the size of the papilla and nanostructures on the composite surfaces is smaller than those for neat PP, the surface roughness of the PP/HNTs composites is substantially higher than that for neat PP. The more rough surfaces can trap more air, which further leads to the increase of the hydrophobic properties. Therefore, it may be derived that HNTs are responsible for the enhancement of hydrophobic properties of PP.

On the basis of these experimental evidences, the possible formation mechanism of the micro-nano binary structures of the PP/HNTs composites is proposed in Scheme 1. After blending HNTs with the PP solution, PP/HNTs mixture dispersions are obtained. Due to the presence of shear force during stirring, HNTs can be uniformly dispersed in PP solution. When the dispersion is casted on the substrates, the solvents evaporate. In the evaporation process, the phase separation occurs and this leads to the formation of polymer-rich phase and polymer-poor phase. HNTs act as nuclei for polymer and this effect is similar to the "precipitator" role of non-solvent. The polymer chains tend to be absorbed or entangled on the surfaces of the nanoparticles. The nucleation mechanism of HNTs to polymer can be attributed to the "epitaxial growth". With further evaporation of the solvent, polymer chains deposit on the initial formed "polymer/nanotube hybrid seed". Due to the gradually enhanced internal tension during this process, the formed microstructures will break into pieces. Meanwhile nanostructures are formed on the microstructure's surfaces because of the contraction of polymer chains. Finally, interconnected micro-papilla structures decorated with nanostructures are obtained. Since the papilla structures are composed of PP and HNTs, therefore they are "hybrid spherulites". Generally, no naked HNTs can be observed on the surfaces of composites due to the wrapping of PP layers on them as shown in the SEM photo and XPS result. The hybrid spherulites lead to the formation of extreme rough surfaces of PP. As a result, the hydrophobicity of the composites is significantly improved compared with smooth PP surface. Although a similar spherulite featured morphology is obtained for the neat PP, the nucleation mechanism for these two systems is different. As for the neat PP, there are not foreign nucleating points. Polymer chains that normally possess a coil conformation and then the other polymer chains absorb and aggregate on this coil, forming the typical spherulite morphology. The mechanism is referred to as homogenous nucleation. However, for the PP/HNTs solutions, the nano fibrillar structure of HNTs provides a 1D nucleation surface for PP chains. HNTs serve as nucleating agents and each HNT has multiple nucleation sites of PP. The homogenous nucleation was prohibited. All the PP crystals epitaxially grow on HNTs under this condition thus nucleated via a heterogeneous nucleation mechanism. It is considered that the heterogeneous nucleation process has a higher crystallization rate than that for the homogenous nucleation. This is reflected in the results of weight loss experiment. The unique micro-nano binary structures enclose large volume of air further lead to lowered sliding angle of the composites surfaces. It should be concluded that the prepared surfaces with PP/HNTs composites demonstrate a similar surface topology with lotus leaves. The artificial lotus leaves surface morphologies of polymer were also observed in the fluorine-end-capped polyurethane/poly(methyl methacrylate) systems [33].

3.4. Thermal degradation stability of PP/HNTs composites

Beside the improved hydrophobic property and lowered cost of PP for superhydrophobic surface applications by HNTs, HNTs can also alter the thermal degradation stability of PP. The influence of HNTs on the degradation behavior of PP in air atmosphere was evaluated by TGA. Fig. 9 presents the TGA curves of PP and its composites in air. As observed in Fig. 9, the TGA curves for the composites shift to high temperature region remarkably which indicates the degradation of PP is substantially restricted by HNTs. However, HNTs can significantly weaken the resistance of PP to thermal-oxidative aging (a much higher carbonyl index for PP/HNTs composites) [34]. Therefore, it seems that these two results are contradictive. This phenomenon can be explained by the different decomposition mechanisms of PP for the two processes. For aging experiment, the aging temperature is lower than 200 °C and the attraction of hydrogen atoms from the PP chains dominates this process [35]. Due to the presence of oxygen, this process leads to the formation of the carbonyl groups. The decomposition of the PP can be initiated by acidic groups on the external surface of the halloysite or by the air entrapped within the tubular lumen. Therefore, HNTs can weaken the resistance of PP to thermal-oxidative aging. For the thermal degradation of PP under a persistent overheating procedure, the breakage of the polymer backbone dominates the process. Due to the formation of hybrid sperulites and the resulted enhanced interfacial bonding for the present PP/HNTs composites, the uniformly dispersed HNTs can protects the polymer from contacting with heat and oxygen during the process of degradation (barrier effects). As a result, the PP/HNTs composites show significantly increased thermal degradation stability.

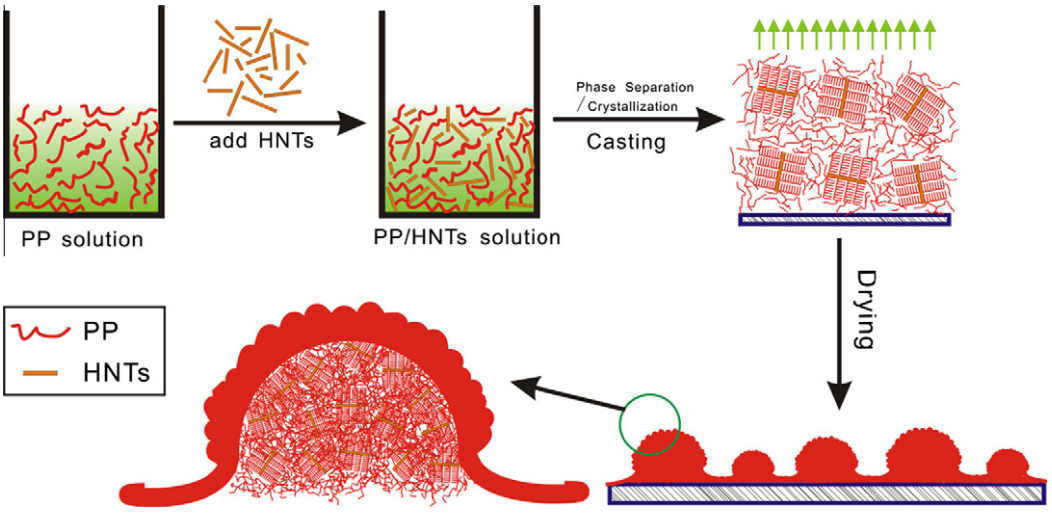

Scheme 1. Schematic representations of the hypothetical mechanism of PP/HNTs hybrid spherulite superstructure formation.

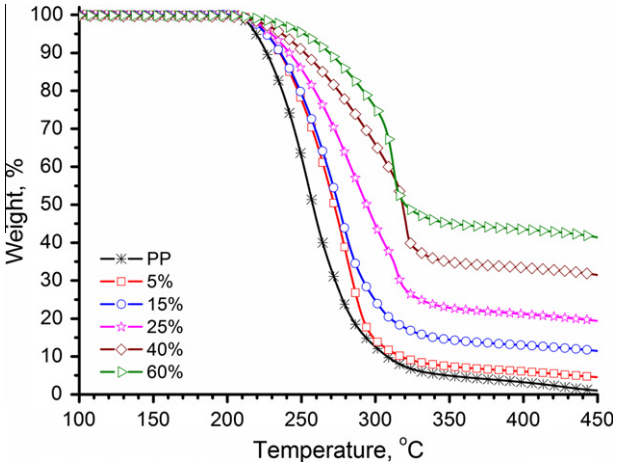

Fig. 9. TGA curves of PP and PP/HNTs composites in air.

4. Conclusions

HNTs are incorporated into PP for tailoring the surface microstructures of the composites prepared by solution casting method. HNTs can accelerate the phase separation process by playing the role of heterogeneous nuclei for PP. This effect leads to formation of micro-papilla like hybrid spherulites with nanostructures on the composite surfaces. The surfaces with micro-nano binary roughness are superhydrophobic with a maximum water contact angle higher than 160° and sliding angle less than 10°. The spherulites size, surface roughness, and wetting property can be tuned by HNTs. HNTs can significantly improve the thermal degradation behavior of PP which is attributed to the well-dispersed HNTs and the strengthened interfacial bonding by nucleation. The present work provides an alternative routine for preparing polymer superhydrophobic surfaces via tailoring the surface microstructures by adding nanoparticles in a solution process. This method can also be used in other polymers/nanoparticles systems for investigating its effectiveness, for example, the polymer/carbon nanotubes systems.

Acknowledgments

We are grateful for the financial support by the National Natural Science Foundation of China with Grant number of 50603005, 50873035 and the Doctorate Foundation of South China University of Technology. The authors also thank Dr. Hau-To Wong for proof reading of the manuscript.

References

[1] T. Onda, S. Shibuichi, Langmuir 19 (1996) 2125.
[2] W. Barthlott, C. Neinhuis, Planta 202 (1997) 1.
[3] L. Feng, S.H. Li, H.J. Li, J. Zhai, Y.L. Song, L. Jiang, D.B. Zhu, Angew. Chem., Int. Ed. 41 (2002) 1221.
[4] A. Lafuma, D. Quere, Nat. Mater. 2 (2003) 457.
[5] R. Blossey, Nat. Mater. 2 (2003) 301.
[6] H.Y. Erbil, A.L. Demirel, Y. Avci, O. Mert, Science 299 (2003) 1377.
[7] X.F. Gao, L. Jiang, Nature 432 (2004) 36.
[8] V.A. Sinani, M.K. Gheith, A.A. Yaroslavov, A.A. Rakhnyanskaya, K. Sun, A.A. Mamedov, J.P. Wicksted, N.A. Kotov, J. Am. Chem. Soc. 127 (2005) 3463.
[9] C. Dorrer, J. Ruhe, Soft Matter 5 (2009) 51.
[10] Y.M. Zheng, X.F. Gao, L. Jiang, Soft Matter 3 (2007) 178.
[11] X. Kang, W.W. Zi, Z.G. Xu, H.L. Zhang, Appl. Surf. Sci. 253 (2007) 8830.
[12] Z.Q. Yuan, H. Chen, J.D. Zhang, D.J. Zhao, Y.J. Liu, X.Y. Zhou, S. Li, P. Shi, J.X. Tang, X. Chen, Sci. Technol. Adv. Mater. 9 (2008) 045007.
[13] Z.Q. Yuan, H. Chen, J.X. Tang, D.J. Zhao, J. Appl. Polym. Sci. 113 (2009) 1626.
[14] N. Zhao, J. Xu, Q.D. Xie, L.H. Weng, X.L. Guo, X.L. Zhang, L.H. Shi, Macromol. Rapid Commun. 26 (2005) 1075.
[15] Y. Zhang, H. Wang, B. Yan, Y.W. Zhang, P. Yin, G.L. Shen, R.Q. Yu, J. Mater. Chem. 18 (2008) 4442.
[16] Y. Wang, Z.M. Liu, B.X. Han, H.X. Gao, J.L. Zhang, X. Kuang, Chem. Commun. (2004) 800.
[17] X.H. Li, G.M. Chen, Y.M. Ma, L. Feng, H.Z. Zhao, L. Jiang, F.S. Wang, Polymer 47 (2006) 506.
[18] J. Shi, N.M. Alves, J.F. Mano, Bioinsp. Biomim. 3 (2008) 034003.
[19] R. Rioboo, M. Voue, A. Vaillant, D. Seveno, J. Conti, A.I. Bondar, D.A. Ivanov, J. De Coninck, Langmuir 24 (2008) 9508.
[20] S.S. Ray, M. Bousmina, Polymer Nanocomposites and Their Applications, American Scientific Publishers, 2006.
[21] C.Y. Li, L.Y. Li, W.W. Cai, S.L. Kodjie, K.K. Tenneti, Adv. Mater. 17 (2005) 1198.
[22] K. Wang, F. Chen, Q. Zhang, Q. Fu, Polymer 49 (2008) 4745.
[23] P. Maiti, P.H. Nam, M. Okamoto, N. Hasegawa, A. Usuki, Macromolecules 35 (2002) 2042.
[24] S.H. Kim, S.H. Ahn, T. Hirai, Polymer 44 (2003) 5625.
[25] M.X. Liu, B.C. Guo, M.L. Du, F. Chen, D.M. Jia, Polymer 50 (2009) 3022.
[26] M.X. Liu, B.C. Guo, M.L. Du, X.J. Cai, D.M. Jia, Nanotechnology 18 (2007) 455703.
[27] N. Pasquini, Polypropylene Handbook, second ed., Hanser Gardner, 2005.
[28] M. Liu, B. Guo, M. Du, D. Jia, Appl. Phys. A 88 (2007) 391.
[29] B.C. Guo, Q.L. Zou, Y.D. Lei, M.L. Du, M.X. Liu, D.M. Jia, Thermochim. Acta 484 (2009) 48.
[30] J.A. Franco, S.E. Kentish, J.M. Perera, G.W. Stevens, J. Membr. Sci. 318 (2008) 107.
[31] R. Wenzel, Ind. Eng. Chem. 28 (1936) 988.
[32] A.B.D. Cassie, S. Baxter, Trans. Faraday Soc. 40 (1944) 546.
[33] Q.D. Xie, J. Xu, L. Feng, L. Jiang, W.H. Tang, X.D. Luo, C.C. Han, Adv. Mater. 16 (2004) 302.
[34] M.L. Du, B.C. Guo, M.X. Liu, D.M. Jia, Polym. Polym. Compos. 15 (2007) 321.
[35] S.H. Hamid, Handbook of Polymer Degradation, second ed., CRC Press, 2000.